

THE B_c MESON AND ITS SCALAR COUSIN WITH THE QCD SUM RULESZhi-Gang Wang¹

Department of Physics, North China Electric Power University, Baoding 071003, P. R. China

Abstract

In the present work, we use optical theorem to calculate the next-to-leading order corrections to the QCD spectral densities directly in the QCD sum rules for the pseudoscalar and scalar B_c mesons. We take the experimental data as guides to perform updated analysis, and obtain the masses and decay constants, especially the decay constants, which are the fundamental input parameters in the high energy physics, therefore the pure leptonic decay widths, which can be confronted to the experimental data in the future.

PACS number: 12.38.Bx, 12.38.Lg

Key words: Next-to-leading order contributions, QCD sum rules

1 Introduction

In 1998, the CDF collaboration observed the pseudoscalar B_c mesons through the semi-leptonic decay modes $B_c^\pm \rightarrow J/\psi \ell^\pm X$ and $B_c^\pm \rightarrow J/\psi \ell^\pm \bar{\nu}_\ell$ in the $p\bar{p}$ collisions at the energy $\sqrt{s} = 1.8$ TeV at the Fermilab Tevatron, the measured mass is $6.40 \pm 0.39 \pm 0.13$ GeV [1, 2]. It is the first time to observe the bottom-charm meson experimentally.

In 2007, the CDF collaboration confirmed the B_c mesons through the non-leptonic decay modes $B_c^\pm \rightarrow J/\psi \pi^\pm$ with the measured mass $6275.6 \pm 2.9 \pm 2.5$ MeV [3]. In 2008, the D0 collaboration reconstructed the non-leptonic decays $B_c^\pm \rightarrow J/\psi \pi^\pm$ and confirmed the B_c mesons with the measured mass $6300 \pm 14 \pm 5$ MeV [4]. Now the B_c meson is well established, the average value listed in the Review of Particle Physics is $6274.47 \pm 0.27 \pm 0.17$ MeV [5].

In 2014, the ATLAS collaboration reported the observation of a structure in the $B_c^\pm \pi^+ \pi^-$ invariant mass spectrum with a significance of 5.2 standard deviations, which is consistent with the predicted B'_c meson with a mass of $6842 \pm 4 \pm 5$ MeV [6].

In 2019, the CMS collaboration observed two excited $\bar{b}c$ states in the $B_c^+ \pi^+ \pi^-$ invariant mass spectrum with a significance exceeding five standard deviations, which are consistent with the B_c^{*+} and $B_c^{\prime+}$, respectively [7]. The two states are separated in mass by $29.1 \pm 1.5 \pm 0.7$ MeV, and the mass of the B_c^{*+} is measured to be $6871.0 \pm 1.2 \pm 0.8 \pm 0.8$ MeV. Also in 2019, the LHCb collaboration observed the excited B_c^{*+} (with a global (local) statistical significance of 2.2σ (3.2σ)) and $B_c^{\prime+}$ (with a global (local) statistical significance of 6.3σ (6.8σ)) mesons in the $B_c^+ \pi^+ \pi^-$ invariant mass spectrum. The B_c^{*+} meson has a mass of $6841.2 \pm 0.6 \pm 0.1 \pm 0.8$ MeV, which is reconstructed without the low-energy photon emitted in the $B_c^{*+} \rightarrow B_c^+ \gamma$ decay following the process $B_c^{*+} \rightarrow B_c^{*+} \pi^+ \pi^-$, while the $B_c^{\prime+}$ meson has a mass of $6872.1 \pm 1.3 \pm 0.1 \pm 0.8$ MeV [8].

It is very odd that the B'_c meson emerges as heavier than the mass of the B_c^{*+} meson, which is in conflict with all the theoretical estimations, this maybe or maybe not due to impossibility of reconstruction of the low-energy photon in the $B_c^{*+} \rightarrow B_c^+ \gamma$ decay [9], more precisely experimental data are still needed. Only the B_c and B'_c mesons are listed in Review of Particle Physics [5], which are in contrary to the copious (well-established) spectroscopy of the charmonium and bottomonium states. Despite the enormous developments on the heavy quark physics in recent years, the bottom-charm spectroscopy remains poorly known, which calls for further investigations.

The beauty-charm mesons provide an optimal laboratory for exploring both the perturbative and nonperturbative dynamics of the heavy quarks, due to absence of the light quark's contamination, and for exploring the strong and electro-weak interactions, as they are composed of two different heavy flavor quarks and cannot annihilate into gluons or photons. For the excited $\bar{c}b$ states, which lie below the BD threshold, would decay into the B_c meson through the radiative

¹ E-mail: zgwang@aliyun.com.

decays or hadronic decays [10, 11], while the ground state B_c can only decay weakly through emitting a virtual W -boson, thus it cannot decay through strong or electromagnetic interactions.

There have been a number of theoretical works on the mass spectroscopy of the bottom-charm mesons, such as the relativized (or relativistic) quark model with an special potential [10, 11, 12, 13, 14], the nonrelativistic quark model with an special potential [15, 16, 17, 18, 19, 20, 21, 22, 23], the semi-relativistic quark model using the shifted large- N expansion [24, 25], the perturbative QCD [26], the nonrelativistic renormalization group [27], the lattice QCD [28, 29, 30, 31], the Bethe-Salpeter equation [32, 33, 34], the full QCD sum rules [35, 36, 37, 38, 39, 40, 41], the potential model combined with the QCD sum rules [15, 16], etc.

With the continuous developments in experimental techniques, we expect that more $c\bar{b}$ states would be observed by the ATLAS, CMS, LHCb, etc in the future. The decay constant, which parameterizes the coupling between a current and a meson, plays an important role in exploring the exclusive processes, because the decay constants are not only a fundamental parameter describing the pure leptonic decays, but also are an universal input parameter related to the distribution amplitudes, form-factors, partial decay widths and branching fractions in many processes. By precisely measuring the branching fractions, we can resort to the decay constants to extract the CKM matrix element in the standard model and search for new physics beyond the standard model [42].

Decay constants of the bottom-charm mesons have been investigated in a number of theoretical approaches, such as the full QCD sum rules [35, 36, 37, 38, 39, 40, 41, 43, 44], the potential model combined with the QCD sum rules [15, 16], the QCD sum rule combined with the heavy quark effective theory [45, 46, 47, 48, 49, 50, 51, 52], the covariant light-front quark model [53, 54], the lattice non-relativistic QCD [31], the shifted large- N expansion method [25], the field correlator method [55], etc. However, the values from different theoretical approaches vary in a large range, it is interesting and necessary to extend our previous works on the vector and axialvector B_c mesons [40] to investigate the pseudoscalar and scalar B_c mesons with the full QCD sum rules by including next-to-leading order radiative corrections and choose the updated input parameters, thus our investigations are performed in a consistent and systematic way. We take the experimental data [5, 6, 7, 8] as guides to choose the suitable Borel parameters and continuum threshold parameters, examine the masses and decay constants of the pseudoscalar and scalar B_c mesons with the full QCD sum rules, therefore we calculate the pure leptonic decay widths to be confronted to the experimental data in the future.

The article is arranged: we calculate the next-to-leading order contributions to the spectral densities and obtain the QCD sum rules in Sect.2; in Sect.3, we present the numerical results and discussions; and Sect.4 is reserved for our conclusions.

2 Explicit calculations of the QCD spectral densities at the next-to-leading order

We write down the two-point correlation functions firstly,

$$\Pi_{P/S}(p^2) = i \int d^4x e^{ip \cdot x} \langle 0 | T \{ J(x) J^\dagger(0) \} | 0 \rangle, \quad (1)$$

where $J(x) = J_P(x)$ and $J_S(x)$,

$$\begin{aligned} J_P(x) &= \bar{c}(x) i \gamma_5 b(x), \\ J_S(x) &= \bar{c}(x) b(x), \end{aligned} \quad (2)$$

the subscripts P and S represent the pseudoscalar and scalar mesons, respectively. The correlation functions can be written in the form,

$$\Pi_{P/S}(p^2) = \frac{1}{\pi} \int_{(m_b+m_c)^2}^{\infty} ds \frac{\text{Im} \Pi_{P/S}(s)}{s - p^2}, \quad (3)$$

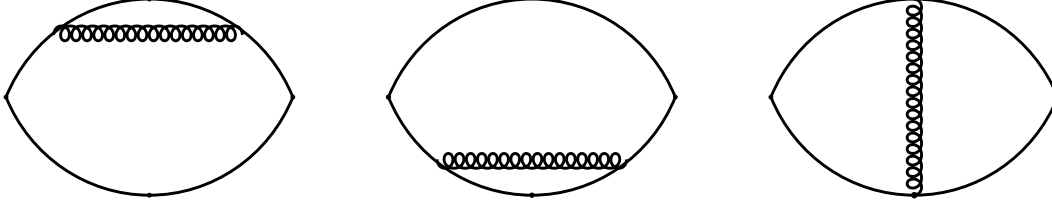


Figure 1: The next-to-leading order contributions to the correlation functions.

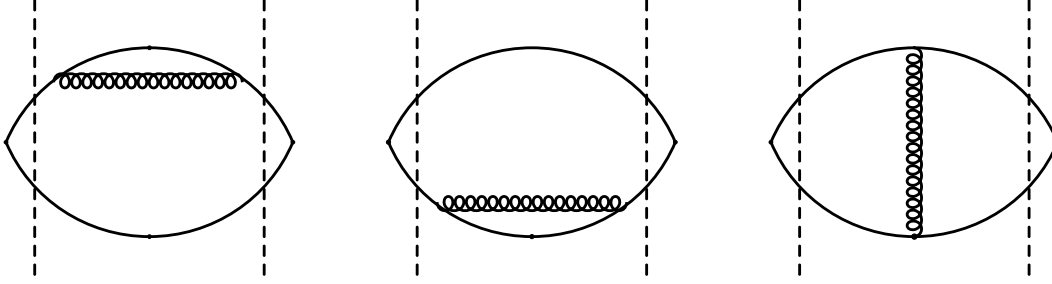


Figure 2: Six possible cuts correspond to virtual gluon emissions.

according to the dispersion relation, where

$$\begin{aligned} \frac{\text{Im}\Pi_{P/S}(s)}{\pi} &= \rho_{P/S}(s) \\ &= \rho_{P/S}^0(s) + \rho_{P/S}^1(s) + \rho_{P/S}^2(s) + \cdots, \end{aligned} \quad (4)$$

the QCD spectral densities $\rho_{P/S}(s)$ are expanded in terms of the strong fine structure constant $\alpha_s = \frac{g_s^2}{4\pi}$, the $\rho_{P/S}^0(s)$, $\rho_{P/S}^1(s)$, $\rho_{P/S}^2(s)$, \cdots are the spectral densities of the leading order, next-to-leading order, and next-to-next-to-leading order, \cdots . At the leading order,

$$\rho_{P/S}^0(s) = \frac{3}{8\pi^2} \frac{\sqrt{\lambda(s, m_b^2, m_c^2)}}{s} [s - (m_b \mp m_c)^2], \quad (5)$$

where the standard phase space factor,

$$\lambda(s, m_b^2, m_c^2) = s^2 + m_b^4 + m_c^4 - 2sm_b^2 - 2sm_c^2 - 2m_b^2m_c^2. \quad (6)$$

At the next-to-leading order, there exist three standard Feynman diagrams, which correspond to the self-energy and vertex corrections respectively, and make contributions to the correlation functions, see Fig.1. We calculate the imaginary parts of those Feynman diagrams resorting to the Cutkosky's rule or optical theorem, the two methods result in the same analytical expressions, then we use dispersion relation to acquire the correlation functions at the quark-gluon level [39, 56]. There exist ten possible cuts, six cuts make attributions to virtual gluon emissions and four cuts make attributions to real gluon emissions.

The six cuts which are shown in Fig.2 make attributions to virtual gluon emissions, and could be classified as the self-energy and vertex corrections, respectively. We calculate the Feynman diagrams straightforwardly by adopting the dimensional regularization to regularize both the ultraviolet and infrared divergences, and resort to the on-shell renormalization scheme to absorb the ultraviolet divergences by accomplishing the wave-function and quark-mass renormalizations. Then we take account of all contributions which are shown in Fig.2 by the simple replacements of

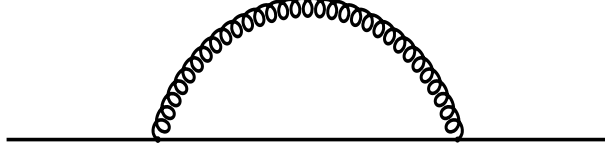


Figure 3: The quark self-energy correction.

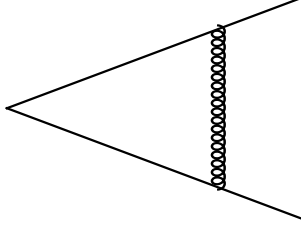


Figure 4: The vertex correction.

the vertexes in all the currents,

$$\begin{aligned}
\bar{u}(p_1)i\gamma_5 u(p_2) &\rightarrow \bar{u}(p_1)i\gamma_5 u(p_2) + \bar{u}(p_1)i\tilde{\Gamma}_5 u(p_2) \\
&= \sqrt{Z_1}\sqrt{Z_2}\bar{u}(p_1)i\gamma_5 u(p_2) + \bar{u}(p_1)i\Gamma_5 u(p_2) \\
&= \bar{u}(p_1)i\gamma_5 u(p_2) \left(1 + \frac{1}{2}\delta Z_1 + \frac{1}{2}\delta Z_2\right) + \bar{u}(p_1)i\Gamma_5 u(p_2), \tag{7}
\end{aligned}$$

$$\begin{aligned}
\bar{u}(p_1)u(p_2) &\rightarrow \bar{u}(p_1)u(p_2) + \bar{u}(p_1)\tilde{\Gamma}_0 u(p_2) \\
&= \sqrt{Z_1}\sqrt{Z_2}\bar{u}(p_1)u(p_2) + \bar{u}(p_1)\Gamma_0 u(p_2) \\
&= \bar{u}(p_1)u(p_2) \left(1 + \frac{1}{2}\delta Z_1 + \frac{1}{2}\delta Z_2\right) + \bar{u}(p_1)\Gamma_0 u(p_2), \tag{8}
\end{aligned}$$

where

$$Z_i = 1 + \delta Z_i = 1 + \frac{4}{3} \frac{\alpha_s}{\pi} \left(-\frac{1}{4\varepsilon_{UV}} + \frac{1}{2\varepsilon_{IR}} + \frac{3}{4} \log \frac{m_i^2}{4\pi\mu^2} + \frac{3}{4}\gamma - 1 \right), \tag{9}$$

is the i quark's wave-function renormalization constant which originates from the self-energy diagram, see Fig.3, and

$$\begin{aligned}
\Gamma_{5/0} &= \gamma_5 \frac{4}{3} g_s^2 \int_0^1 dx \int_0^{1-x} dy \int \frac{d^D k_E}{(2\pi)^D} \\
&\quad \frac{\Gamma(3)}{[k_E^2 + (xp_1 + yp_2)^2]^3} \left\{ 4k_E^2 \left(1 - \frac{1}{2}\varepsilon_{UV}\right) + 2(1-x-y+2xy)(s - m_b^2 - m_c^2) \right. \\
&\quad \left. \pm 2(x+y)m_b m_c + 2x(1-2x)m_b^2 + 2y(1-2y)m_c^2 \right\}, \tag{10}
\end{aligned}$$

for the vertex diagrams after accomplishing the Wick's rotation, see Fig.4, where the γ is the Euler constant, the μ is the energy scale of renormalization, and the $k_E = (k_1, k_2, k_3, k_4)$ is Euclidean four-momentum. We set the dimension $D = 4 - 2\varepsilon_{UV} = 4 + 2\varepsilon_{IR}$ to regularize the ultraviolet and infrared divergences respectively, where the ε_{UV} and ε_{IR} are positive dimension-less quantities, and we would add the energy scale factors $\mu^{2\varepsilon_{UV}}$ or $\mu^{-2\varepsilon_{IR}}$ if necessary.

We accomplish all the integrals over all the variables, and observe that the ultraviolet divergences $\frac{1}{\varepsilon_{\text{UV}}}$ in the $\Gamma_{5/0}$, δZ_1 and δZ_2 are canceled out completely with each other, the offsets are warranted by the Ward identity. So the total contributions do not have ultraviolet divergences,

$$\begin{aligned}\tilde{\Gamma}_5 &= \frac{4}{3} \frac{\alpha_s}{4\pi} \gamma_5 f_P(s), \\ \tilde{\Gamma}_0 &= \frac{4}{3} \frac{\alpha_s}{4\pi} f_S(s),\end{aligned}\tag{11}$$

where

$$\begin{aligned}f_{P/S}(s) &= \bar{f}_{P/S}(s) + \frac{2}{\varepsilon_{\text{IR}}} + 3 \log \frac{m_b m_c}{4\pi\mu^2} + 4 \log \frac{4\pi\mu^2}{s} - \gamma + 4 - \frac{2(s - m_b^2 - m_c^2)}{\sqrt{\lambda(s, m_b^2, m_c^2)}} \log \left(\frac{1+\omega}{1-\omega} \right) \\ &\quad \left(\frac{1}{\varepsilon_{\text{IR}}} + \log \frac{s}{4\pi\mu^2} + \gamma \right), \\ \bar{f}_{P/S}(s) &= 4\bar{V}(s) + 2(s - m_b^2 - m_c^2) [\bar{V}_{00}(s) - V_{10}(s) - V_{01}(s) + 2V_{11}(s)] \pm 2m_b m_c \\ &\quad [V_{10}(s) + V_{01}(s)] + 2m_b^2 [V_{10}(s) - 2V_{20}(s)] + 2m_c^2 [V_{01}(s) - 2V_{02}(s)], \\ \omega &= \sqrt{\frac{s - (m_b + m_c)^2}{s - (m_b - m_c)^2}},\end{aligned}\tag{12}$$

and $s = p^2$, the definitions and explicit expressions of the notations $\bar{V}(s)$, $\bar{V}_{00}(s)$ and $V_{ij}(s)$ with $i, j = 0, 1, 2$ are given in the appendix.

The contributions of all the virtual gluon emissions to the imaginary parts of the Feynman diagrams in Fig.1 are,

$$\frac{\text{Im}\Pi_{P/S}^V(s)}{\pi} = \frac{4}{3} \frac{\alpha_s}{4\pi} \frac{6}{\pi} \int \frac{d^{D-1}\vec{p}_1}{(2\pi)^{D-1}2E_{p_1}} \frac{d^{D-1}\vec{p}_2}{(2\pi)^{D-1}2E_{p_2}} (2\pi)^D \delta^D(p - p_1 - p_2) f(s) [s - (m_b \mp m_c)^2],\tag{13}$$

the superscript V denotes the virtual gluon emissions. We accomplish all the integrals straightforwardly in the dimension $D = 4 + 2\varepsilon_{\text{IR}}$ as there does not exist ultraviolet divergence, and obtain the analytical expressions,

$$\begin{aligned}\frac{\text{Im}\Pi_{P/S}^V(s)}{\pi} &= \frac{4}{3} \frac{\alpha_s}{\pi} \rho_{P/S}^0(s) \left\{ \frac{1}{\varepsilon_{\text{IR}}} - 2 \log 4\pi + \frac{1}{2} \gamma + \frac{1}{2} \log \frac{\lambda^2(s, m_b^2, m_c^2) m_b^3 m_c^3}{\mu^8 s^3} + \frac{1}{2} \bar{f}_{P/S}(s) \right. \\ &\quad \left. - \frac{s - m_b^2 - m_c^2}{\sqrt{\lambda(s, m_b^2, m_c^2)}} \log \left(\frac{1+\omega}{1-\omega} \right) \left[\frac{1}{\varepsilon_{\text{IR}}} - 2 \log 4\pi + 2\gamma - 2 + \log \frac{\lambda(s, m_b^2, m_c^2)}{\mu^4} \right] \right\}.\end{aligned}\tag{14}$$

The four cuts in the Feynman diagrams shown in Fig.5 only make contributions to the real gluon emissions, the corresponding scattering amplitudes are shown explicitly in Fig.6. From the two diagrams in Fig.6, we write down the scattering amplitudes $T_{5,\alpha}^a(p)$ and $T_{0,\alpha}^a(p)$,

$$\begin{aligned}T_{5,\alpha}^a(p) &= \bar{u}(p_1) \left\{ ig_s \frac{\lambda^a}{2} \gamma_\alpha \frac{i}{\not{p}_1 + \not{k} - m_b} i\gamma_5 + i\gamma_5 \frac{i}{-\not{p}_2 - \not{k} - m_c} ig_s \frac{\lambda^a}{2} \gamma_\alpha \right\} v(p_2), \\ T_{0,\alpha}^a(p) &= \bar{u}(p_1) \left\{ ig_s \frac{\lambda^a}{2} \gamma_\alpha \frac{i}{\not{p}_1 + \not{k} - m_b} + \frac{i}{-\not{p}_2 - \not{k} - m_c} ig_s \frac{\lambda^a}{2} \gamma_\alpha \right\} v(p_2),\end{aligned}\tag{15}$$

where the λ^a is the Gell-Mann matrix. Then we obtain the contributions to the imaginary parts

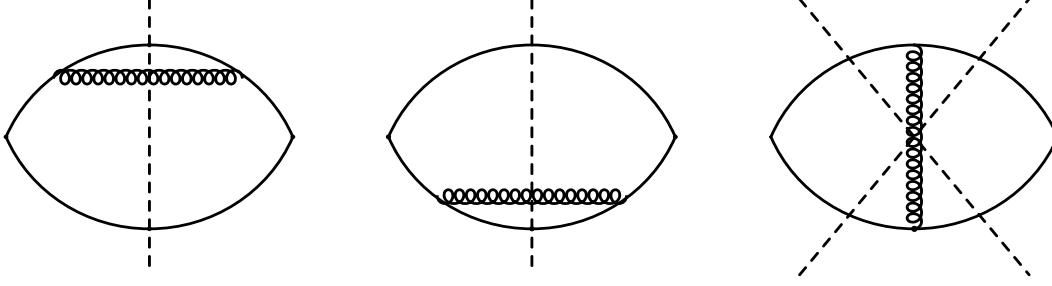


Figure 5: Four possible cuts correspond to real gluon emissions.

of the Feynman diagrams with the optical theorem,

$$\begin{aligned}
\frac{\text{Im}\Pi_{P/S}^R(s)}{\pi} &= -\frac{1}{2\pi} \int \frac{d^{D-1}\vec{k}}{(2\pi)^{D-1}2E_k} \frac{d^{D-1}\vec{p}_1}{(2\pi)^{D-1}2E_{p_1}} \frac{d^{D-1}\vec{p}_2}{(2\pi)^{D-1}2E_{p_2}} (2\pi)^D \delta^D(p - k - p_1 - p_2) \\
&\quad \text{Tr} \left\{ T_{5/0,\alpha}^a(p) T_{5/0,\beta}^{a\dagger}(p) \right\} g^{\alpha\beta} \\
&= -\frac{2g_s^2}{\pi} \int \frac{d^{D-1}\vec{k}}{(2\pi)^{D-1}2E_k} \frac{d^{D-1}\vec{p}_1}{(2\pi)^{D-1}2E_{p_1}} \frac{d^{D-1}\vec{p}_2}{(2\pi)^{D-1}2E_{p_2}} (2\pi)^D \delta^D(p - k - p_1 - p_2) \\
&\quad \left\{ 2 \left[s - (m_b \mp m_c)^2 \right] \left[\frac{m_b^2}{(k \cdot p_1)^2} + \frac{m_c^2}{(k \cdot p_2)^2} - \frac{s - m_b^2 - m_c^2}{k \cdot p_1 k \cdot p_2} \right. \right. \\
&\quad \left. \left. + \frac{s - K^2}{k \cdot p_1 k \cdot p_2} \right] - \frac{(s - K^2)^2}{k \cdot p_1 k \cdot p_2} \right\}, \tag{16}
\end{aligned}$$

where we have used the formulas $\sum u(p_1)\bar{u}(p_1) = \not{p}_1 + m_b$ and $\sum v(p_2)\bar{v}(p_2) = \not{p}_2 - m_c$ for the quark and antiquark respectively, and we introduce the symbol $K^2 = (p_1 + p_2)^2$ for simplicity, and introduce the superscript R to denote the real gluon emissions. We accomplish the integrals in the dimension $D = 4 + 2\varepsilon_{\text{IR}}$ because there only exist the infrared divergences (no ultraviolet divergences), and obtain the contributions,

$$\begin{aligned}
\frac{\text{Im}\Pi_{P/S}^R(s)}{\pi} &= \frac{4}{3} \frac{\alpha_s}{\pi} \rho_{P/S}^0(s) \left\{ -\frac{1}{\varepsilon_{\text{IR}}} + 2 \log 4\pi - 2\gamma + 2 - \log \frac{\lambda^3(s, m_b^2, m_c^2)}{m_b^2 m_c^2 s^2 \mu^4} + (s - m_b^2 - m_c^2) \bar{R}_{12}(s) \right. \\
&\quad \left. - \bar{R}_{11}(s) - \bar{R}_{22}(s) - R_{12}^1(s) + \frac{R_{12}^2}{2} \frac{1}{s - (m_b \mp m_c)^2} + \frac{s - m_b^2 - m_c^2}{\sqrt{\lambda(s, m_b^2, m_c^2)}} \right. \\
&\quad \left. \log \left(\frac{1+\omega}{1-\omega} \right) \left[\frac{1}{\varepsilon_{\text{IR}}} - 2 \log 4\pi + 2\gamma - 2 + \log \frac{\lambda^3(s, m_b^2, m_c^2)}{m_b^2 m_c^2 s^2 \mu^4} \right] \right\}, \tag{17}
\end{aligned}$$

the definitions and explicit expressions of the $\bar{R}_{11}(s)$, $\bar{R}_{22}(s)$, $\bar{R}_{12}(s)$, $R_{12}^1(s)$ and $R_{12}^2(s)$ are given in the appendix.

Now we obtain the total QCD spectral densities at the next-to-leading order,

$$\begin{aligned}
\rho_{P/S}^1(s) &= \frac{4}{3} \frac{\alpha_s}{\pi} \rho_{P/S}^0(s) \left\{ \frac{1}{2} \bar{f}_{P/S}(s) - \bar{R}_{11}(s) - \bar{R}_{22}(s) - R_{12}^1(s) + (s - m_b^2 - m_c^2) \bar{R}_{12}(s) \right. \\
&\quad \left. + \frac{R_{12}^2}{2} \frac{1}{s - (m_b \mp m_c)^2} - \frac{3}{2} \gamma + 2 + \frac{1}{2} \log \frac{m_b^7 m_c^7 s}{\lambda^4(s, m_b^2, m_c^2)} \right. \\
&\quad \left. + \frac{s - m_b^2 - m_c^2}{\sqrt{\lambda(s, m_b^2, m_c^2)}} \log \left(\frac{1+\omega}{1-\omega} \right) \log \frac{\lambda^2(s, m_b^2, m_c^2)}{m_b^2 m_c^2 s^2} \right\}. \tag{18}
\end{aligned}$$

The infrared divergences of the forms $\frac{1}{\varepsilon_{\text{IR}}}$, $\log \left(\frac{1+\omega}{1-\omega} \right) \frac{1}{\varepsilon_{\text{IR}}}$ from the virtual and real gluon emissions are canceled out with each other completely, the offsets are guaranteed by the Lee-Nauenberg

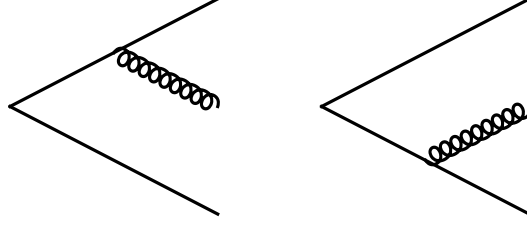


Figure 6: The amplitudes for the real gluon emissions.

theorem [57]. The analytical expressions are applicable in many phenomenological analysis besides the QCD sum rules.

Then we calculate the contributions of the gluon condensate directly, the calculations are easy and no much to say. Finally, we obtain the analytical expressions of the QCD spectral densities, take the quark-hadron duality below the continuum thresholds $s_{P/S}^0$ and perform the Borel transforms in regard to the variable $P^2 = -p^2$ to acquire the QCD sum rules,

$$\frac{f_{P/S}^2 M_{P/S}^4}{(m_b \pm m_c)^2} \exp\left(-\frac{M_{P/S}^2}{T^2}\right) = \int_{(m_b+m_c)^2}^{s_{P/S}^0} ds \left[\rho_{P/S}^0(s) + \rho_{P/S}^1(s) + \rho_{P/S}^{\text{con}}(s) \right] \exp\left(-\frac{s}{T^2}\right), \quad (19)$$

where

$$\begin{aligned} \rho_{P/S}^{\text{con}}(s) = & \mp \frac{m_b m_c}{24T^4} \langle \frac{\alpha_s GG}{\pi} \rangle \int_0^1 dx \left[\frac{m_c^2}{x^3} + \frac{m_b^2}{(1-x)^3} \right] \delta(s - \tilde{m}_Q^2) \\ & \pm \frac{m_b m_c}{8T^2} \langle \frac{\alpha_s GG}{\pi} \rangle \int_0^1 dx \left[\frac{1}{x^2} + \frac{1}{(1-x)^2} \right] \delta(s - \tilde{m}_Q^2) \\ & - \frac{s}{24T^4} \langle \frac{\alpha_s GG}{\pi} \rangle \int_0^1 dx \left[\frac{(1-x)m_c^2}{x^2} + \frac{xm_b^2}{(1-x)^2} \right] \delta(s - \tilde{m}_Q^2), \end{aligned} \quad (20)$$

$\tilde{m}_Q^2 = \frac{m_b^2}{1-x} + \frac{m_c^2}{x}$, the T^2 is the Borel parameter, and the decay constants are defined by,

$$\begin{aligned} \langle 0 | J_P(0) | P(p) \rangle &= \frac{f_P M_P^2}{m_b + m_c}, \\ \langle 0 | J_S(0) | S(p) \rangle &= \frac{f_S M_S^2}{m_b - m_c}, \end{aligned} \quad (21)$$

in other words,

$$\begin{aligned} \langle 0 | J_A^\alpha(0) | P(p) \rangle &= i f_P p^\alpha, \\ \langle 0 | J_V^\alpha(0) | S(p) \rangle &= i f_S p^\alpha, \end{aligned} \quad (22)$$

the subscripts A and V denote the axial-vector and vector currents, respectively.

We eliminate the decay constants $f_{P/S}$ and obtain the QCD sum rules for the masses of the pseudoscalar and scalar B_c mesons,

$$M_{P/S}^2 = \frac{\int_{(m_b+m_c)^2}^{s_{P/S}^0} ds \frac{d}{d(-1/T^2)} \left[\rho_{P/S}^0(s) + \rho_{P/S}^1(s) + \rho_{P/S}^{\text{con}}(s) \right] \exp\left(-\frac{s}{T^2}\right)}{\int_{(m_b+m_c)^2}^{s_{P/S}^0} ds \left[\rho_{P/S}^0(s) + \rho_{P/S}^1(s) + \rho_{P/S}^{\text{con}}(s) \right] \exp\left(-\frac{s}{T^2}\right)}. \quad (23)$$

3 Numerical results and discussions

The value of the gluon condensate $\langle \frac{\alpha_s GG}{\pi} \rangle$ has been updated from time to time, and changes greatly, we adopt the updated value $\langle \frac{\alpha_s GG}{\pi} \rangle = 0.022 \pm 0.004 \text{ GeV}^4$ [58]. We take the \overline{MS} masses of the heavy quarks $m_c(m_c) = 1.275 \pm 0.025 \text{ GeV}$ and $m_b(m_b) = 4.18 \pm 0.03 \text{ GeV}$ from the Particle Data Group [5]. In addition, we take account of the energy-scale dependence of the \overline{MS} masses,

$$\begin{aligned} m_Q(\mu) &= m_Q(m_Q) \left[\frac{\alpha_s(\mu)}{\alpha_s(m_Q)} \right]^{\frac{12}{33-2n_f}}, \\ \alpha_s(\mu) &= \frac{1}{b_0 t} \left[1 - \frac{b_1 \log t}{b_0^2 t} + \frac{b_1^2 (\log^2 t - \log t - 1) + b_0 b_2}{b_0^4 t^2} \right], \end{aligned} \quad (24)$$

where $t = \log \frac{\mu^2}{\Lambda^2}$, $b_0 = \frac{33-2n_f}{12\pi}$, $b_1 = \frac{153-19n_f}{24\pi^2}$, $b_2 = \frac{2857 - \frac{5033}{9}n_f + \frac{325}{27}n_f^2}{128\pi^3}$, $\Lambda = 213 \text{ MeV}$, 296 MeV and 339 MeV for the quark flavor numbers $n_f = 5, 4$ and 3 , respectively [5]. We choose $n_f = 4$ and 5 for the c and b quarks, respectively, and then evolve all the heavy quark masses to the typical energy scale $\mu = 2 \text{ GeV}$.

The lower threshold $(m_b + m_c)^2$ in the QCD sum rules in Eq.(19) decreases quickly with increase of the energy scale, the energy scale should be larger than 1.7 GeV , which corresponds to the squared mass of the B_c meson, 39.4 GeV^2 . If we take the typical energy scale $\mu = 2 \text{ GeV}$, which corresponds to the lower threshold $(m_b + m_c)^2 \approx 36.0 \text{ GeV}^2 < M_P^2$, it is reasonable and feasible to choose such a particular energy scale.

The experimental masses of the B_c and B'_c mesons are $6274.47 \pm 0.27 \pm 0.17 \text{ MeV}$ and $6871.2 \pm 1.0 \text{ MeV}$ respectively from the Particle Data Group [5]. The scalar B_c meson still escapes the experimental detection, roughly speaking, the theoretical mass is $6712 \pm 18 \pm 7 \text{ MeV}$ from the lattice QCD [30] or 6714 MeV from the nonrelativistic quark model [23]. We can tentatively take the continuum threshold parameters as $s_P^0 = (39 - 47) \text{ GeV}^2$ and $s_S^0 = (45 - 55) \text{ GeV}^2$, and search for the ideal values by assuming the energy gap between the ground state and first radial excited states is about 0.6 GeV , if lacking experimental data; we always resort to such an assumption in the QCD sum rules.

After trial and error, we obtain the ideal Borel windows and continuum threshold parameters, and the corresponding pole contributions about $(70 - 85)\%$, the pole dominance is well satisfied. On the other hand, the gluon condensate plays a tiny important role, the operator product expansion is well convergent. It is reliable to extract the masses and pole residues, which are shown in Table 1 and Figs.7-8.

The predicted mass $M_P = 6.274 \pm 0.054 \text{ GeV}$ is in very good agreement with the experimental data $6274.47 \pm 0.27 \pm 0.17 \text{ MeV}$ from the Particle Data Group [5], while the predicted mass $M_S = 6.702 \pm 0.060 \text{ GeV}$ is consistent with other theoretical calculations [10, 11, 12, 13, 14, 15, 16, 18, 19, 20, 21, 22, 23, 28, 29, 30, 32, 33, 34].

Combined with our previous work [40], we can observe that there exist the relations $\sqrt{s_V^0} - M_V \approx \sqrt{s_P^0} - M_P \approx 0.4 \text{ GeV}$ and $\sqrt{s_A^0} - M_A \approx \sqrt{s_S^0} - M_S \approx 0.6 \text{ GeV}$. Usually, we expect that the energy gaps between the ground states and first radial excitations are about 0.6 GeV . In practical calculations, we can set the continuum threshold parameter $\sqrt{s_0}$ to be any values between the ground state and first radial excitation, i.e. $M_{1S} + \frac{\Gamma_{1S}}{2} < \sqrt{s_0} < M_{2S} - \frac{\Gamma_{2S}}{2}$, if good QCD sum rules can be obtained, where the $1S$ and $2S$ stand for the ground state and first radial excitation, respectively. The energy gaps 0.4 GeV and 0.6 GeV are all make sense.

As for the decay constants, even for the pseudoscalar B_c meson, the theoretical values vary in a large range, for example, the values from the full QCD sum rules (QCDSR) [16, 36, 37, 41, 43, 44], the relativistic quark model (RQM) [11, 12], the non-relativistic quark model (NRQM) [18, 19], the light-front quark model (LFQM) [54], the lattice non-relativistic QCD (LNQCD) [31], the shifted N -expansion method (SNEM) [25], the field correlator method (FCM) [55], the Bethe-Salpeter equation (BSE) [33], etc; and we present those values in Table 2 for clearness. At the present time, it is difficult to say which value is superior to others.

	$T^2(\text{GeV}^2)$	$s_0(\text{GeV}^2)$	pole	$M(\text{GeV})$	$f(\text{GeV})$
$B_c(0^-)$	$3.0 - 4.0$	44 ± 1	$(68 - 89)\%$	6.274 ± 0.054	0.371 ± 0.037
$B_c(0^+)$	$5.4 - 6.4$	54 ± 1	$(69 - 83)\%$	6.702 ± 0.060	0.236 ± 0.017
$\hat{B}_c(0^-)$	$2.4 - 3.4$	44 ± 1	$(75 - 94)\%$	6.275 ± 0.045	0.208 ± 0.015
$\hat{B}_c(0^+)$	$3.5 - 4.5$	54 ± 1	$(85 - 96)\%$	6.704 ± 0.055	0.119 ± 0.006

Table 1: The Borel windows, continuum threshold parameters, pole contributions, masses and decay constants of the pseudoscalar and scalar B_c mesons, where the $\hat{}$ denotes that the radiative $\mathcal{O}(\alpha_s)$ corrections have been neglected.

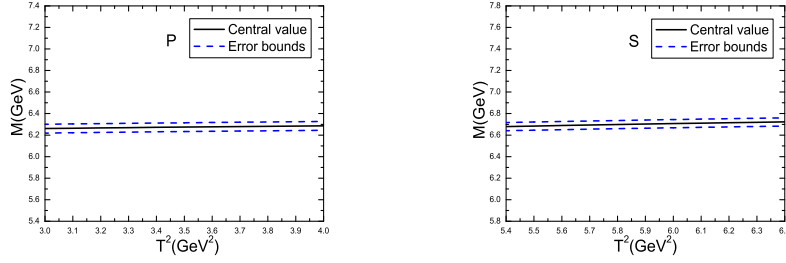


Figure 7: The masses of the pseudoscalar (P) and scalar (S) B_c mesons with variations of the Borel parameters T^2 .

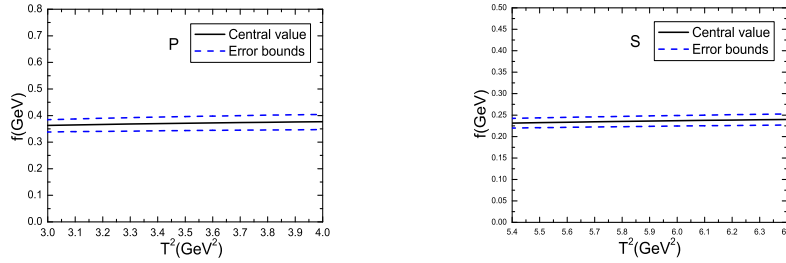


Figure 8: The decay constants of the pseudoscalar (P) and scalar (S) B_c mesons with variations of the Borel parameters T^2 .

	$f_P(\text{MeV})$	References
QCDSR	460 ± 60	[16]
QCDSR	300 ± 65	[36]
QCDSR	360 ± 60	[37]
QCDSR	270 ± 30	[41]
QCDSR	371 ± 17	[43]
QCDSR	528 ± 19	[44]
QCDSR	371 ± 37	This work
RQM	410 ± 40	[11]
RQM	433	[12]
NRQM	498	[18]
NRQM	440	[19]
LFQM	523 ± 62	[54]
LNQCD	420 ± 13	[31]
LNEM	315^{+26}_{-50}	[25]
FCM	438 ± 10	[55]
BSE	322 ± 42	[33]

Table 2: The decay constant of the pseudoscalar B_c meson from different theoretical works.

The present prediction $f_P = 371 \pm 37$ MeV is in very good agreement with the value 371 ± 17 MeV from the full QCD sum rules [43]. In our previous work, we obtain the values $f_V = 384 \pm 32$ MeV and $f_A = 373 \pm 25$ MeV for the vector and axial-vector B_c mesons, respectively [40]. Our calculations indicate that $f_P \approx f_V \approx f_A > f_S$. While in the QCD sum rule combined with the heavy quark effective theory up to the order α_s^3 , the decay constants have the relations $\tilde{f}_P = f_P > f_V > f_S > \tilde{f}_S > f_A$ [47], where the decay constants \tilde{f}_P and \tilde{f}_S are defined by

$$\begin{aligned}\langle 0|J_P(0)|P(p)\rangle &= \tilde{f}_P M_P, \\ \langle 0|J_S(0)|S(p)\rangle &= \tilde{f}_S M_S.\end{aligned}\tag{25}$$

From Eq.(21) and Eq.(25), we can obtain the relations,

$$\begin{aligned}\tilde{f}_P &= f_P \frac{M_P}{m_b + m_c}, \\ \tilde{f}_S &= f_S \frac{M_S}{m_b - m_c},\end{aligned}\tag{26}$$

it is obvious that $\tilde{f}_P > f_P$ and $\tilde{f}_S < f_S$, which are in contrary to the relations obtained in Ref.[47], so no definite conclusion can be obtained. Naively, we expect that the vector mesons have larger decay constants than the corresponding pseudoscalar mesons [59].

If we neglect the radiative $\mathcal{O}(\alpha_s)$ corrections (in other words, the next-to-leading order contributions), the same input parameters would lead to too large hadron masses, we have to choose the energy scales $\mu = 2.1$ GeV and 2.2 GeV for the pseudoscalar and scalar B_c mesons, respectively. Then we refit the Borel parameters, the corresponding pole contributions, masses and decay constants are given explicitly in Table 1. From the Table, we can see explicitly that the predicted masses change slightly, while the predicted decay constants change greatly, the decay constants without the radiative $\mathcal{O}(\alpha_s)$ corrections only count for about 56% of the corresponding ones with the radiative $\mathcal{O}(\alpha_s)$ corrections. The radiative $\mathcal{O}(\alpha_s)$ corrections play an important role, we should take it into account.

The pure leptonic decay widths $\Gamma_{\ell\bar{\nu}_\ell}$ of the pseudoscalar and scalar B_c mesons can be written

as,

$$\Gamma_{\ell\bar{\nu}_\ell} = \frac{G_F^2}{8\pi} |V_{bc}|^2 f_{P/S}^2 M_{P/S} M_\ell^2 \left(1 - \frac{M_\ell^2}{M_{P/S}^2}\right)^2, \quad (27)$$

where the leptons $\ell = e, \mu, \tau$, the Fermi constant $G_F = 1.16637 \times 10^{-5} \text{ GeV}^{-2}$, the CKM matrix element $V_{cb} = 40.8 \times 10^{-3}$, the masses of the leptons $m_e = 0.511 \times 10^{-3} \text{ GeV}$, $m_\mu = 105.658 \times 10^{-3} \text{ GeV}$, $m_\tau = 1776.86 \times 10^{-3} \text{ GeV}$, the life time of the B_c meson $\tau_{B_c} = 0.510 \times 10^{-12} \text{ s}$ from the Particle Data Group [5]. We take the masses and decay constants of the pseudoscalar and scalar B_c mesons from the QCD sum rules to obtain the partial decay widths,

$$\begin{aligned} \Gamma_{P \rightarrow e\bar{\nu}_e} &= 2.03 \times 10^{-12} \text{ eV}, \\ \Gamma_{P \rightarrow \mu\bar{\nu}_\mu} &= 8.68 \times 10^{-8} \text{ eV}, \\ \Gamma_{P \rightarrow \tau\bar{\nu}_\tau} &= 2.08 \times 10^{-5} \text{ eV}, \\ \Gamma_{S \rightarrow e\bar{\nu}_e} &= 8.78 \times 10^{-13} \text{ eV}, \\ \Gamma_{S \rightarrow \mu\bar{\nu}_\mu} &= 3.75 \times 10^{-8} \text{ eV}, \\ \Gamma_{S \rightarrow \tau\bar{\nu}_\tau} &= 9.18 \times 10^{-6} \text{ eV}, \end{aligned} \quad (28)$$

and the branching fractions,

$$\begin{aligned} \text{Br}_{P \rightarrow e\bar{\nu}_e} &= 1.57 \times 10^{-9}, \\ \text{Br}_{P \rightarrow \mu\bar{\nu}_\mu} &= 6.73 \times 10^{-5}, \\ \text{Br}_{P \rightarrow \tau\bar{\nu}_\tau} &= 1.61 \times 10^{-2}. \end{aligned} \quad (29)$$

The largest branching fractions of the $B_c(0^-) \rightarrow \ell\bar{\nu}_\ell$ are of the order 10^{-2} , the tiny branching fractions maybe escape experimental detections. By precisely measuring the branching fractions, we can examine the theoretical calculations strictly, although it is a hard work.

4 Conclusion

In this work, we extend our previous works on the vector and axialvector B_c mesons to investigate the pseudoscalar and scalar B_c mesons with the full QCD sum rules by including next-to-leading order corrections and choose the updated input parameters. In calculating the next-to-leading order corrections, we use optical theorem (or Cutkosky's rule) to obtain the QCD spectral densities straightforwardly, and resort to the dimensional regularization to regularize both the ultraviolet and infrared divergences, which are canceled out with each other separately, the total QCD spectral densities have neither ultraviolet divergences nor infrared divergences. Then we calculate the gluon condensate contributions and reach the QCD sum rules. We take the experimental data as guides to choose the suitable Borel parameters and continuum threshold parameters, and make reasonable predictions for the masses and decay constants, therefore the pure leptonic decay widths, which can be confronted to the experimental data in the future to examine the theoretical calculations or extract the decay constants, which are fundamental input parameters in the high energy physics.

Acknowledgements

This work is supported by National Natural Science Foundation, Grant Number 12175068.

Appendix

At first, we write down all the elementary integrals involving the vertex corrections,

$$\begin{aligned} V_{ab}(s) &= 16\pi^2 \int_0^1 dx \int_0^{1-x} dy \int \frac{d^D k_E}{(2\pi)^D} \frac{x^a y^b \Gamma(3)}{[k_E^2 + (xp_1 + yp_2)^2]^3}, \\ V(s) &= 16\pi^2 \left(1 - \frac{1}{2}\varepsilon_{\text{UV}}\right) \int_0^1 dx \int_0^{1-x} dy \int \frac{d^D k_E}{(2\pi)^D} \frac{k_E^2 \Gamma(3)}{[k_E^2 + (xp_1 + yp_2)^2]^3}, \end{aligned} \quad (30)$$

and accomplish all the integrals to acquire the analytical expressions,

$$\begin{aligned} V_{00}(s) &= \frac{1}{\sqrt{\lambda(s, m_b^2, m_c^2)}} \left\{ -\log\left(\frac{1+\omega}{1-\omega}\right) \left(\frac{1}{\varepsilon_{\text{IR}}} + \log \frac{s}{4\pi\mu^2} + \gamma\right) + \frac{\log^2(1-\omega_1^2)}{4} - \log^2(1+\omega_1) \right. \\ &\quad \left. + \frac{\log^2(1-\omega_2^2)}{4} - \log^2(1+\omega_2) + 2\log(\omega_1 + \omega_2) \log\left(\frac{1+\omega}{1-\omega}\right) - \log\omega_1 \log\left(\frac{1+\omega_2}{1-\omega_2}\right) \right. \\ &\quad \left. - \log\omega_2 \log\left(\frac{1+\omega_1}{1-\omega_1}\right) - \text{Li}_2\left(\frac{2\omega_1}{1+\omega_1}\right) - \text{Li}_2\left(\frac{2\omega_2}{1+\omega_2}\right) + \pi^2 \right\}, \\ &= \bar{V}_{00}(s) - \frac{1}{\sqrt{\lambda(s, m_b^2, m_c^2)}} \log\left(\frac{1+\omega}{1-\omega}\right) \left(\frac{1}{\varepsilon_{\text{IR}}} + \log \frac{s}{4\pi\mu^2} + \gamma\right), \\ V_{10}(s) &= \frac{1}{s} \left\{ \frac{1}{2} \log\left(\frac{1-\omega_1^2}{1-\omega_2^2}\right) - \frac{1}{\omega_2} \log\left(\frac{1+\omega}{1-\omega}\right) + \log \frac{\omega_2}{\omega_1} \right\}, \\ V_{01}(s) &= V_{10}(s)|_{\omega_1 \leftrightarrow \omega_2}, \\ V_{20}(s) &= \frac{1}{2s} \left\{ -\frac{\omega_1\omega_2}{\omega_1 + \omega_2} \log\left(\frac{1+\omega}{1-\omega}\right) - \frac{\omega_1}{\omega_2(\omega_1 + \omega_2)} \log\left(\frac{1+\omega}{1-\omega}\right) + \frac{\omega_1}{\omega_1 + \omega_2} \log\left(\frac{1-\omega_1^2}{1-\omega_2^2}\right) \right. \\ &\quad \left. + \frac{2\omega_1}{\omega_1 + \omega_2} \log \frac{\omega_2}{\omega_1} + 1 \right\}, \\ V_{02}(s) &= V_{20}(s)|_{\omega_1 \leftrightarrow \omega_2}, \\ V_{11}(s) &= \frac{1}{2s} \left\{ \frac{\omega_1\omega_2}{\omega_1 + \omega_2} \log\left(\frac{1+\omega}{1-\omega}\right) - \frac{\omega_1 - \omega_2}{2(\omega_1 + \omega_2)} \log\left(\frac{1-\omega_1^2}{1-\omega_2^2}\right) - \frac{1}{\omega_1 + \omega_2} \log\left(\frac{1+\omega}{1-\omega}\right) \right. \\ &\quad \left. + \frac{\omega_1}{\omega_1 + \omega_2} \log \frac{\omega_1}{\omega_2} + \frac{\omega_2}{\omega_1 + \omega_2} \log \frac{\omega_2}{\omega_1} - 1 \right\}, \\ V(s) &= \frac{1}{\varepsilon_{\text{UV}}} + \log \frac{4\pi\mu^2}{s} - \gamma + 2 - \frac{2\omega_1\omega_2}{\omega_1 + \omega_2} \log\left(\frac{1+\omega}{1-\omega}\right) - \frac{\omega_2}{\omega_1 + \omega_2} \log(1-\omega_1^2) \\ &\quad - \frac{\omega_1}{\omega_1 + \omega_2} \log(1-\omega_2^2) - 2 \frac{\omega_1 \log \omega_1 + \omega_2 \log \omega_2}{\omega_1 + \omega_2} + 2\log(\omega_1 + \omega_2), \\ &= \bar{V}(s) + \frac{1}{\varepsilon_{\text{UV}}} + \log \frac{4\pi\mu^2}{s} - \gamma + 2, \end{aligned} \quad (31)$$

where

$$\begin{aligned} \omega_1 &= \frac{\sqrt{\lambda(s, m_b^2, m_c^2)}}{s + m_b^2 - m_c^2}, \\ \omega_2 &= \frac{\sqrt{\lambda(s, m_b^2, m_c^2)}}{s + m_c^2 - m_b^2}, \\ M &= \frac{m_b + m_c}{m_b - m_c}, \\ \text{Li}_2(x) &= -\int_0^x dt \frac{\log(1-t)}{t}. \end{aligned} \quad (32)$$

Then we introduce the notation

$$\int dps = \int \frac{d^{D-1}\vec{k}}{2E_k} \frac{d^{D-1}\vec{p}_1}{2E_{p_1}} \frac{d^{D-1}\vec{p}_2}{2E_{p_2}} \delta^D(p - k - p_1 - p_2),$$

for simplicity, and write down the elementary three-body phase-space integrals,

$$\begin{aligned} R_{11}(s) &= \frac{sm_b^2}{\pi^2 \sqrt{\lambda(s, m_b^2, m_c^2)}} (2\pi)^{-4\varepsilon_{\text{IR}}} \mu^{-2\varepsilon_{\text{IR}}} \int dps \frac{1}{(k \cdot p_1)^2} \\ &= \frac{1}{2\varepsilon_{\text{IR}}} - \log 4\pi + \gamma - 1 + \log \frac{\sqrt{\lambda(s, m_b^2, m_c^2)}^3}{m_b m_c s \mu^2} - \frac{s + m_b^2 - m_c^2}{2\sqrt{\lambda(s, m_b^2, m_c^2)}} \log \left(\frac{1 + \omega_1}{1 - \omega_1} \right) \\ &\quad - \frac{m_b^2 - m_c^2}{\sqrt{\lambda(s, m_b^2, m_c^2)}} \log \left(\frac{1 + \omega_1}{1 - \omega_1} \right) - \frac{s - m_b^2 + m_c^2}{\sqrt{\lambda(s, m_b^2, m_c^2)}} \log \left(\frac{1 + \omega}{1 - \omega} \right) \\ &= \bar{R}_{11}(s) + \frac{1}{2\varepsilon_{\text{IR}}} - \log 4\pi + \gamma - 1 + \log \frac{\sqrt{\lambda(s, m_b^2, m_c^2)}^3}{m_b m_c s \mu^2}, \\ R_{22}(s) &= R_{11}(s)|_{m_b \leftrightarrow m_c}, \\ R_{12}(s) &= \frac{s}{\pi^2 \sqrt{\lambda(s, m_b^2, m_c^2)}} (2\pi)^{-4\varepsilon_{\text{IR}}} \mu^{-2\varepsilon_{\text{IR}}} \int dps \frac{1}{k \cdot p_1 k \cdot p_2} \\ &= \frac{1}{\sqrt{\lambda(s, m_b^2, m_c^2)}} \left\{ \log \left(\frac{1 + \omega}{1 - \omega} \right) \left[\frac{1}{\varepsilon_{\text{IR}}} - 2 \log 4\pi + 2\gamma - 2 + 2 \log \frac{\sqrt{\lambda(s, m_b^2, m_c^2)}^3}{m_b m_c s \mu^2} \right] \right. \\ &\quad - 2 \log \frac{m_b}{m_c} \log \left(\frac{M + \omega}{M - \omega} \right) - \log^2 \left(\frac{1 + \omega}{1 - \omega} \right) + 2 \log \frac{s}{\bar{s}} \log \left(\frac{1 + \omega}{1 - \omega} \right) - 4 \text{Li}_2 \left(\frac{2\omega}{1 + \omega} \right) \\ &\quad + 2 \text{Li}_2 \left(\frac{\omega - 1}{\omega - M} \right) + 2 \text{Li}_2 \left(\frac{\omega - 1}{\omega + M} \right) - 2 \text{Li}_2 \left(\frac{\omega + 1}{\omega - M} \right) - 2 \text{Li}_2 \left(\frac{\omega + 1}{\omega + M} \right) - \frac{1}{2} \text{Li}_2 \left(\frac{1 + \omega_1}{2} \right) \\ &\quad \left. - \frac{1}{2} \text{Li}_2 \left(\frac{1 + \omega_2}{2} \right) - \text{Li}_2(\omega_1) - \text{Li}_2(\omega_2) + \frac{\log 2 \log [(1 + \omega_1)(1 + \omega_2)]}{2} - \frac{\log^2 2}{2} + \frac{\pi^2}{12} \right\}, \\ &= \bar{R}_{12}(s) + \frac{1}{\sqrt{\lambda(s, m_b^2, m_c^2)}} \log \left(\frac{1 + \omega}{1 - \omega} \right) \left[\frac{1}{\varepsilon_{\text{IR}}} - 2 \log 4\pi + 2\gamma - 2 + 2 \log \frac{\sqrt{\lambda(s, m_b^2, m_c^2)}^3}{m_b m_c s \mu^2} \right], \\ R_{12}^1(s) &= \frac{s}{\pi^2 \sqrt{\lambda(s, m_b^2, m_c^2)}} \int dps \frac{s - K^2}{k \cdot p_1 k \cdot p_2} \\ &= \frac{s}{\sqrt{\lambda(s, m_b^2, m_c^2)}} \left\{ \log^2(1 - \omega) - \log^2(1 + \omega) + 2 \log \frac{2s}{\bar{s}} \log \left(\frac{1 + \omega}{1 - \omega} \right) + 2 \text{Li}_2 \left(\frac{1 - \omega}{2} \right) \right. \\ &\quad \left. - 2 \text{Li}_2 \left(\frac{1 + \omega}{2} \right) + 2 \text{Li}_2 \left(\frac{1 + \omega}{1 + M} \right) + 2 \text{Li}_2 \left(\frac{1 + \omega}{1 - M} \right) - 2 \text{Li}_2 \left(\frac{1 - \omega}{1 - M} \right) - 2 \text{Li}_2 \left(\frac{1 - \omega}{1 + M} \right) \right\}, \\ R_{12}^2(s) &= \frac{s}{\pi^2 \sqrt{\lambda(s, m_b^2, m_c^2)}} \int dps \frac{(s - K^2)^2}{k \cdot p_1 k \cdot p_2} \\ &= \frac{s^2}{\sqrt{\lambda(s, m_b^2, m_c^2)}} \left\{ \log^2(1 - \omega) - \log^2(1 + \omega) + 2 \log \frac{4s}{\bar{s}} \log \left(\frac{1 + \omega}{1 - \omega} \right) + 2 \text{Li}_2 \left(\frac{1 - \omega}{2} \right) \right. \\ &\quad - 2 \text{Li}_2 \left(\frac{1 + \omega}{2} \right) + 2 \text{Li}_2 \left(\frac{1 + \omega}{1 + M} \right) + 2 \text{Li}_2 \left(\frac{1 + \omega}{1 - M} \right) - 2 \text{Li}_2 \left(\frac{1 - \omega}{1 - M} \right) - 2 \text{Li}_2 \left(\frac{1 - \omega}{1 + M} \right) \\ &\quad \left. + \frac{2\omega\bar{s}}{s} - \frac{\bar{s}}{s} (1 + \omega^2) \log \left(\frac{1 + \omega}{1 - \omega} \right) \right\}, \tag{33} \end{aligned}$$

where $\bar{s} = s - (m_b - m_c)^2$.

References

- [1] F. Abe et al, Phys. Rev. **D58** (1998) 112004.
- [2] F. Abe et al, Phys. Rev. Lett. **81** (1998) 2432.
- [3] T. Aaltonen et al, Phys. Rev. Lett. **100** (2008) 182002.
- [4] V. M. Abazov et al, Phys. Rev. Lett. **101** (2008) 012001.
- [5] R. L. Workman et al, Prog. Theor. Exp. Phys. **2022** (2022) 083C01.
- [6] G. Aad et al, Phys. Rev. Lett. **113** (2014) 212004.
- [7] A. M. Sirunyan et al, Phys. Rev. Lett. **122** (2019) 132001.
- [8] R. Aaij et al, Phys. Rev. Lett. **122** (2019) 232001.
- [9] Z. G. Wang, Eur. Phys. J. **C73** (2013) 2559.
- [10] S. Godfrey and N. Isgur, Phys. Rev. **D32** (1985) 189.
- [11] S. Godfrey, Phys. Rev. **D70** (2004) 054017.
- [12] D. Ebert, R. N. Faustov and V. O. Galkin, Phys. Rev. **D67** (2003) 014027.
- [13] S. N. Gupta and J. M. Johnson, Phys. Rev. **D53** (1996) 312.
- [14] J. Zeng, J. W. Van Orden and W. Roberts, Phys. Rev. **D52** (1995) 5229.
- [15] S. S. Gershtein, V. V. Kiselev, A. K. Likhoded and A. V. Tkabladze, Phys. Rev. **D51** (1995) 3613.
- [16] S. S. Gershtein, V. V. Kiselev, A. K. Likhoded and A. V. Tkabladze, Phys. Usp. **38** (1995) 1.
- [17] E. J. Eichten and C. Quigg, Phys. Rev. **D49** (1994) 5845.
- [18] E. J. Eichten and C. Quigg, Phys. Rev. **D99** (2019) 054025.
- [19] A. P. Monteiro, M. Bhat and K. B. V. Kumar, Int. J. Mod. Phys. **A32** (2017) 1750021.
- [20] L. P. Fulcher, Phys. Rev. **D60** (1999) 074006.
- [21] N. R. Soni, B. R. Joshi, R. P. Shah, H. R. Chauhan and J. N. Pandya, Eur. Phys. J. **C78** (2018) 592.
- [22] P. G. Ortega, J. Segovia, D. R. Entem and F. Fernandez, Eur. Phys. J. **C80** (2020) 223.
- [23] Q. Li, M. S. Liu, L. S. Lu, Q. F. Lu, L. C. Gui and X. H. Zhong, Phys. Rev. **D99** (2019) 096020.
- [24] S. M. Ikhdaire and R. Sever, Int. J. Mod. Phys. **A19** (2004) 1771.
- [25] S. M. Ikhdaire and R. Sever, Int. J. Mod. Phys. **A21** (2006) 6699.
- [26] N. Brambilla and A. Vairo, Phys. Rev. **D62** (2000) 094019.
- [27] A. A. Penin, A. Pineda, V. A. Smirnov and M. Steinhauser, Phys. Lett. **B593** (2004) 124.
- [28] E. B. Gregory et al, Phys. Rev. Lett. **104** (2010) 022001.
- [29] C. T. H. Davies et al, Phys. Lett. **B382** (1996) 131.

- [30] N. Mathur, M. Padmanath and S. Mondal, Phys. Rev. Lett. **121** (2018) 202002.
- [31] B. D. Jones and R. M. Woloshyn, Phys. Rev. **D60** (1999) 014502.
- [32] A. A. El-Hady, M. A. K. Lodhi and J. P. Vary, Phys. Rev. **D59** (1999) 094001.
- [33] G. L. Wang, Phys. Lett. **B650** (2007) 15.
- [34] G. L. Wang, T. Wang, Q. Li and C. H. Chang, JHEP **05** (2022) 006.
- [35] E. Bagan, H. G. Dosch, P. Gosdzinsky, S. Narison and J. M. Richard, Z. Phys. **C64** (1994) 57.
- [36] M. Chabab, Phys. Lett. **B325** (1994) 205.
- [37] P. Colangelo, G. Nardulli and N. Paver, Z. Phys. **C57** (1993) 43.
- [38] V. V. Kiselev and A. V. Tkabladze, Phys. Rev. **D48** (1993) 5208.
- [39] Z. G. Wang, Acta Phys. Polon. **B44** (2013) 1971.
- [40] Z. G. Wang, Eur. Phys. J. **A49** (2013) 131.
- [41] T. M. Aliev, T. Barakat and S. Bilmis, Nucl. Phys. **B947** (2019) 114726.
- [42] M. Blanke et al, Phys. Rev. **D99** (2019) 075006.
- [43] S. Narison, Phys. Lett. **B802** (2020) 135221.
- [44] M. J. Baker, J. Bordes, C. A. Dominguez, J. Penarrocha and K. Schilcher, JHEP **07** (2014) 032.
- [45] A. I. Onishchenko and O. L. Veretin, Eur. Phys. J. **C50** (2007) 801.
- [46] J. Lee, W. L. Sang and S. Kim, JHEP **01** (2011) 113.
- [47] W. Tao and Z. J. Xiao, arXiv: 2310.17500 [hep-ph].
- [48] W. Tao, R. L. Zhu and Z. J. Xiao, Phys. Rev. **D106** (2022) 114037.
- [49] W. Tao, R. L. Zhu and Z. J. Xiao, Eur. Phys. J. **C83** (2023) 294.
- [50] L. B. Chen and C. F. Qiao, Phys. Lett. **B748** (2015) 443.
- [51] W. L. Sang, H. F. Zhang and M. Z. Zhou, Phys. Lett. **B839** (2023) 137812.
- [52] F. Feng, Y. Jia, Z. Mo, J. Pan, W. L. Sang and J. Y. Zhang, arXiv: 2208.04302 [hep-ph].
- [53] R. C. Verma, J. Phys. **G39** (2012) 025005.
- [54] S. Tang, Y. Li, P. Maris and J. P. Vary, Phys. Rev. **D98** (2018) 114038.
- [55] A. M. Badalian, B. L. G. Bakker and Yu. A. Simonov, Phys. Rev. **D75** (2007) 116001.
- [56] L. J. Reinders, H. Rubinstein and S. Yazaki, Phys. Rept. **127** (1985) 1.
- [57] T. D. Lee and M. Nauenberg, Phys. Rev. **133** (1964) B1549.
- [58] S. Narison, Phys. Lett. **B706** (2012) 412.
- [59] Z. G. Wang, Eur. Phys. J. **C75** (2015) 427.